THERMOMECHANICAL BEHAVIOR OF SINGLE CRYSTALLINE TANTALUM IN THE STATIC AND DYNAMIC REGIME

D. Rittel [1*], M.L. Silva [2], B. Poon [2] and G. Ravichandran [2]

[1] Faculty of Mechanical Engineering, Technion, 32000 Haifa, Israel
[2] Graduate Aerospace Laboratories, California Institute of Technology, Pasadena, CA 91125, USA

ABSTRACT

This paper reports the thermomechanical behavior of single crystalline tantalum (Ta) in the [100] and [110] orientations. Mechanical testing was carried out at low and high strain rates using a Kolsky bar together with the simultaneous recording of the specimen's temperature by means of an infrared detector. The results show a marked difference in terms of flow curve and strain hardening between the two orientations, irrespective of the strain-rate. Similarly, the thermomechanical behavior, namely the efficiency of the thermomechanical conversion at high strain-rates (β_{int}), is observed to be different for each orientation. A comparison of the present results with those obtained for pure polycrystalline Ta (Rittel et al., 2007) reveals some similarity of flow curves with the [100] orientation. By contrast, the [110] orientation is observed to possess β_{int} characteristics that are similar to those of the polycrystalline material. These results are presented and discussed, thus completing the overall experimental characterization of this material in order to enable the simulation and validation of the dynamic behavior of polycrystalline Ta on the basis of its single-crystal characteristics.

* Corresponding author: *merittel@technion.ac.il*

I. INTRODUCTION

One of the key ingredients of the numerical simulations of polycrystalline materials is a sound knowledge of the mechanical properties of the single crystal. This information is necessary to test the assumptions that are made in the polycrystalline averaging scheme (Bronkhorst et al., 2007). The literature contains many reports on the quasi-static mechanical properties of single crystals. By contrast, much less is known about the high strain-rate (dynamic) behavior of single crystals. Among those, one may consider tantalum (Ta) which is a typical body-centered cubic crystal, for which the quasi-static mechanical properties and slip systems are well documented (Ferriss et al., 1962; Hartley, 1964; Mitchell and Spitzig, 1965; Mordike and Rudolph, 1967). By contrast, much less is known in the dynamic regime for this material, with the exception of Kapoor and Nemat-Nasser's work on its latent hardening properties (1998b). In parallel, one may find numerous examples of the characterization of pure and slightly alloyed polycrystalline tantalum, e.g. in (Kothari and Anand, 1998; Rittel et al., 2007). If thermomechanical aspects are considered, namely the nature and extent of thermomechanical coupling effects in this material (Farren and Taylor, 1925; Taylor and Quinney, 1934), one can find two reports showing that to a first approximation, the whole of the plastic work is dissipated in the form of heat in the dynamic regime (Kapoor and Nemat-Nasser, 1998a; Rittel et al., 2007). However, this observation pertains to polycrystalline tantalum (and its W-alloy), while there is no equivalent report for the single crystalline material. Here, one may note in passing the scarcity of thermomechanical data of this kind for single crystalline materials in general.

Consequently, the purpose of this paper is to report and discuss the measured mechanical response of pure single crystalline Ta in the quasi-static and the dynamic regimes, together with a detailed characterization of the thermomechanical coupling effects (Bronkhorst et al., 2005; Mason et al., 1994; Rittel, 1999). Throughout this work, a comparison will be made with available results on polycrystalline Ta in order to outline the relevant factors in the micro to macro transition.

The paper is therefore organized as follows. The material and experimental conditions are described in the first section. The next section presents results on the quasi-static mechanical behavior. The third section concentrates on the dynamic response of single crystal Ta, along with the transient temperature measurements. The results are then

discussed, emphasizing the relevance of the single crystal data to the polycrystalline behavior as well as new aspects of the collected thermomechanical data. This section is followed by concluding remarks.

II. MATERIALS AND EXPERIMENTAL

II.1 Materials

High purity (99.99%) single crystals of Ta were purchased from Goodfellow Corporation. Two orientations were selected, [110] and [100]. The near-cylindrical shaped cylinders were of nominal diameters 12mm [110] and 6 mm [100], and 100 mm total length per orientation. Near-cylindrical specimens were sectioned using wire electro-discharge machining with a length of 6 mm for each orientation. A total of 16 specimens were machined per orientation. Since the cross-section of the specimens was not exactly cylindrical but slightly oval, an average diameter was determined for each specimen, based on the arithmetic average of 3 measurements. The loading directions are perpendicular to the orientation (planes), namely (110) and (100). For single crystal Ta, three families of slip systems are reported, namely $\{110\}\langle 111\rangle; \{121\}\langle 111\rangle; \{231\}\langle 111\rangle$.

II.2 Experimental

Quasi-static tests

Compression tests were conducted at room temperature on a servo-hydraulic machine (MTS Model No. 11019), under displacement control. The specimens were compressed by means of cylindrical maraging steel rods. The stress was determined from the force transducer in the machine and the cross sectional area of the samples. The strain was measured using a clip on axial extensometer that was affixed on the steel rods. We also accounted for compliance of the loading device when determining the strain in the sample.

Dynamic tests

The dynamic compression experiments were carried out on a 19.05 mm diameter Kolsky bar made of C300 Maraging steel. Data was reduced according to the well known equations relating the stresses and strains to the incident, reflected and

transmitted strain signals. Wave dispersion was corrected too, according to the guidelines of Lifshitz and Leber (1994) by means of a home-made software ("Twobar"). Finally, specimen equilibrium (usually assumed, but not necessarily verified) was carefully verified in each test, by comparing the applied forces on each side of the specimen.

Transient temperature measurement

Transient temperature measurement was carried out using two systems simultaneously. The first setup was a high speed infrared array camera (FLIR SC6000) recording the temperature of the sample at 1000 fps. This camera recorded the post test temperature rise of the sample after the initial stress wave impacts and resulting deformation. There are several temperature ranges that have calibrations available for the thermal camera. We chose between 30-150ºC and 60-200ºC ranges. The thermal camera is a full field detection system, and as such it does not allow for transient measurements at the microsecond time scale, except for very special cases as in Zehnder et al. (2000). While the sampling rate is considerably lower (of the order of 10^3 fps), interesting observations can still be made of the specimen temperature as it flies away from its initial position. At such a stage, the specimen is likely to have experienced repeated impacts from the stress wave, so that it is considerably hotter than after the first impact which is the only time interval of interest to the infrared (and mechanical) measurement. The second setup, to be briefly described, has been used in the past (Rittel et al., 2007; Rittel et al., 2006) and consists of an infrared detector. The infrared radiometric setup consists of a parabolic mirror and a single element, liquid N2 cooled HgCdTe detector, and its matching amplifier (Judson PA-100). Since a single detector was used, the temperature of a small area can be measured. The size of this area depends on the active area of the detector, which is 100 μm by 100 μm in this case. The imaging system (Newtonian) comprises the parabolic mirror with a radius of curvature of 70 mm, and a 45^0 reflecting flat mirror placed at the focus of the parabolic mirror. The area magnification was set to approximately 1.

In order to determine the temperature of the gauge section from the infrared signal, a small K-type thermocouple was tightly inserted at mid thickness of a typical cylindrical specimen. The calibration procedure of the infrared detector consisted of heating the specimen in a separate furnace, inserting it rapidly between the bars, and simultaneously recording the signal from the thermocouple and that of the infrared detector, as the

specimen cooled down to room temperature. The calibrations were repeated several times, right before dynamic testing, to insure repeatability. Considerable care was exercised concerning accurate and repeatable specimen positioning between the bars, as well as accurate focusing of the IR system on the gauge section. The issue of defocusing, as a result of the dynamic bulging of the specimen was not observed to alter the results, following intentional defocusing tests of the system, noting that the recorded signal was not affected. This observation stands in accord with the results of Regev and Rittel (2008). Moreover, it is well known that some surface texture may develop during the deformation process, which affects the optical characteristics of the investigated material. This eventuality was also taken into account by Kapoor and Nemat-Nasser (1998a). However, due to the scarcity of specimens, we did not look into this aspect of the thermal measurement, assuming that its influence, if any, will be the same for all the tests, so that identified trends will not be affected.

III RESULTS

Quasi-static compression

Typical results of the quasi-static tests are shown in Figure 1 for the two orientations, for various strain rates. A first observation is that the hardening characteristics of the two directions are markedly different. While the [100] exhibits significant strain (parabolic) hardening, irrespective of the strain rate, [110] is considerably softer, with its hardening characteristics reminiscent of stages I and II. In terms of yield stress, the difference between the two orientations seems to be minor. However, the two directions exhibit significant strain-rate sensitivity in the quasi-static regime. Young's modulus can be estimated from the curves, and found to be $\mathrm{E}_{[100]} = 149 \pm 50\,\mathrm{GPa}$, and $\mathrm{E}_{[110]} = 106 \pm 25\,\mathrm{GPa}$. These values can be compared with those found in the literature (Hartley, 1964), namely $\mathrm{E}_{[100]} = 194\,\mathrm{GPa}$ and $E_{[110]} = 147\,GPa$. The agreement is overall reasonable, keeping in mind that the ultrasonic measurements reported in the literature are always more accurate than those based on strain gauge systems.

Figure 1 also shows, for reference, the stress-strain curve of annealed polycrystalline Ta at $\dot{\varepsilon} \approx 10^{-3}\,\mathrm{s}^{-1}$. This flow curve is closer to that of the [100] at a comparable strain rate, although it exhibits different hardening characteristics. At the same time, the hardening behavior of [110] is close to the polycrystalline.

Dynamic compression

Typical results for the dynamic compressive tests are shown in Figure (2), for the two orientations and also for the pure polycrystalline Ta (Rittel et al., 2007). This figure shows one more time the marked difference between the two orientations. [110] is again definitely weaker than [100], and each direction retains its specific tendency for strain hardening, [110] still exhibiting an apparently higher degree of strain-hardening. However, the difference appears to be milder than that observed in the quasi-static regime, which may be the result of thermal softening. One can also note that the mechanical response of the polycrystalline Ta is again much closer to that of the [100] direction than that of [110], at a comparable strain-rate.

The strain-rate sensitivity of each orientation is illustrated in Figure (3) showing the flow stress at $\varepsilon = 0.1$ for the two orientations and polycrystalline Ta. From this figure, it clearly appears that the rate-sensitivity of pure polycrystalline Ta follows closely that of the [100] orientation.

Figure (4) shows the [100] crystals before and after dynamic deformation. The crystals whose cross section was initially almost circular become heavily oblong as a result of the impact test, keeping in mind that this is the result of repeated impacts on the specimen which may remain trapped between the bars before flying off. Such a heavily anisotropic response was not observed for the [110] specimens, which retained their almost circular cross section upon impact.

Temperature evolution

Calibration of the infrared detector

A typical calibration consists of letting the specimen cool down from a given initial temperature, while simultaneously recording the infrared signal and that of a core-thermocouple, and plotting the first as a function of the second. This calibration must be repeated several times, as it suffers from an inherent degree of variability, so that a convincing set of similar curves is obtained. From this point, a representative (average) relationship is fitted to process any future recording. Moreover, the repeatability of the curve is tested by performing random calibrations during the series of tests. This procedure was carried out for the two sets of orientations.

Figure (5) shows the evolution of the temperature with strain for the two orientations tested at different strain rates. It is observed that the temperature rise is rather similar for the 2 orientations, and it also seems to be quite insensitive to the strain rate, in the

investigated range. One should note that a similar observation was made for the polycrystalline Ta (Rittel et al., 2007). The thermal evolution of polycrystalline Ta has been superimposed in Figure (5) at a comparable strain rate. For small strains ($\varepsilon \le 0.1$), the thermal response of the single crystals is virtually identical to that of the polycrystal. However, at larger strains, the recorded temperature of the polycrystal is markedly higher that that of the single crystals.

In order to gain additional insight, one can plot the thermomechanical conversion efficiency factor - β_{int} (Rittel, 1999) - as a function of the plastic strain for each orientation. As shown in Figure (6), two clear groups of data emerge, as a function of the crystalline orientation. For the [100], one finds that $0.4 \le \beta_{int} \le 0.6$. On the other hand, for the [110], $0.8 \le \beta_{int} \le 1.0$. Again, it is interesting to compare with the characteristics of a polycrystal, for which it was measured that $\beta_{int} \approx 1.0$ (Kapoor and Nemat-Nasser, 1998a; Rittel et al., 2007). Therefore a clear trend emerges from this set of data, namely that the thermal behavior of the polycrystalline Ta is closer to that of [110] than that of [100]. This is to be compared with the opposite trend that was observed for the mechanical properties of the single crystals. To rationalize this observation, consider the balance of energy (assuming adiabatic conditions):

$$\beta_{int} \int_0^{\varepsilon_f} \sigma_{ij} d\varepsilon_{ij}^p = \rho C_p \Delta T \qquad (1)$$

Since the same ΔT was obtained for each orientation, the "weaker" [110] direction will yield a higher β_{int}. Here too, one can claim that to a first approximation, β_{int} of the single crystals is both strain-rate independent and tends to a constant range of values from relatively small plastic strains and thereon. Average representative values would be $\beta_{int}[100] = 0.5$ and $\beta_{int}[110] = 0.9$.

The thermal camera recorded the temperature rise in the sample after the initial stress wave impacts, as shown in Figure (7). The temperature distribution and evolution was recorded in the sample. We chose the lower temperature range in order to capture the initial temperature rise as best as possible. The temperature in the first frame within the calibration range used correlates well with the signal from the single element, liquid N2 cooled HgCdTe detector. The successive frames show the increased temperature rise and continued deformation and rigid body motion of the sample. Such figures are seldom recorded for this kind of experiments. Indeed, the thermal camera is much too

slow to capture a full field description in the time window of the infrared detector, but it definitely provides a clear picture of the maximum temperature that can be reached in such a test, mostly when post-mortem observations of the microstructure are of interest. In the present case, the maximum temperature can reach twice the value recorded during the first impact, as it is understood that the specimen is repeatedly impacted by the trapped stress waves in the bars until it finally takes off.

IV DISCUSSION

This paper represents an effort to characterize the thermomechanical response of single crystals of Ta over a variety of strain rates, while keeping in mind the behavior of the polycrystalline material which could be calculated using an averaging scheme. Two different orientations have been selected, which by no means represent the whole range of the available slip systems for this material. Another limitation is that latent hardening has not been addressed in the current work.

With these limitations in mind, the main results of the work can be summarized as follows. From a purely mechanical point of view, the two investigated orientations differ widely in terms of strain hardening, while both are strain rate sensitive. One can distinguish a "strong" [100] orientation as compared to a "weaker" [110]. The strain rate sensitivity and relative strength advantage is maintained for [110] over the whole range of investigated strain rates. It is also interesting to note that from a macroscopic point of view, the mechanical response of polycrystalline Ta is much closer to that of [100] than to [110]. From a practical point of view, this result means that [100] and its latent systems play a dominant role in the mechanical response of polycrystalline Ta, of a kind that should be identified in numerical simulations. In that respect, this observation would greatly simplify the numerical effort required to perform a micro-macro numerical simulation.

The thermal response of single crystals has been seldom investigated and no data is available for Ta in the literature. The temperature rise, as a result of thermomechanical coupling seems to be isotropic, based on the current set of observations (Figure 5). In parallel, the experiments show that the β_{int} factor depends on the orientation, a fact that was not previously noted, although it is expectable. From the two investigated orientations, the "weaker" [110] contributes to higher values of β_{int}, which tend to the value of 1 observed for the polycrystalline material. In other words, [110] being

"softer", it stores less microstructural energy that [100] and therefore dissipates more heat, contributing to a higher β_{int}.

To summarize the current work, two orientations have been systematically investigated. The "stronger" [100] dominates the mechanical response of the polycrystal, while the "weaker" [110] dictates its thermal response. These results should be useful to test numerical averaging schemes.

V CONCLUSIONS

[100] and [110] single crystals of pure Ta have been tested over a wide range of strain-rates, from the quasi-static to the dynamic regime. The evolution of the specimen's temperature was simultaneously monitored and the results were discussed in terms of the previously characterized polycrystalline behavior.

1. The two directions exhibit different flow curves beyond a common yield stress level, and both are strain rate sensitive with distinctly different hardening characteristics.

2.From a mechanical point of view, [100] dominates the mechanical response and brings it close to that of pure polycrystalline Ta.

3. The temperature rise of the single crystals is independent of the orientation and the strain-rate, in the investigated range.

4. The efficiency of the thermomechanical conversion (β_{int}) is dominated by the "weaker" [110] orientation which tends to behave as the polycrystalline material.

5. The present results could serve as benchmarks for numerical simulations of the polycrystalline behavior of Ta.

Acknowledgement

The authors gratefully acknowledge the support of the US Department of Energy through Caltech's PSAAP Center for the Predictive Modeling and Simulation of High-Energy Density Dynamic Response of Materials.

BIBLIOGRAPHY

Bronkhorst, C.A., Hansen, B.L., Cerreta, E.K., Bingert, J.F., 2007. Modeling the microstructural evolution of metallic polycrystalline materials under localization conditions. Journal of the Mechanics and Physics of Solids 55, 2351-2383.

Bronkhorst, C.A., Maudlin, P.J., Cerreta, E.K., Mason, T.A., III, G.T.G., 2005. Shear localization in tantalum top hat samples, Los Alamos national Laboratory: Theoretical Division Nuclear Weapons Highlights 2004-2005, pp. 90-91.

Farren, W.S., Taylor, G.I., 1925. The heat developed during plastic extension of metals. Proc. R. Soc. A107, 422-451.

Ferriss, D.P., Rose, R.M., Wulff, J., 1962. Deformation of tantalum single crystals. Trans. AIME, 975-980.

Hartley, C.S., 1964. Elasticity of tantalum single crystals. J. of the less-common metals 6, 245-248.

Kapoor, R., Nemat-Nasser, S., 1998a. Determination of temperature rise during high strain rate deformation. Mechanics of Materials 27, 1-12.

Kapoor, R., Nemat-Nasser, S., 1998b. High-rate deformation of single crystal tantalum: Temperature dependence and latent hardening. Scripta Materialia 40, 159-164.

Kothari, M., Anand, L., 1998. Elasto-viscoplastic constitutive equations for polycrystalline metals: Applications to tantalum. Journal of the Mechanics and Physics of Solids 46, 51-+.

Lifshitz, J.M., Leber, H., 1994. Data processing in the split Hopkinson pressure bar tests. Int. J. Impact Engng. 15, 723-733.

Mason, J.J., Rosakis, A.J., Ravichandran, G., 1994. On the strain and strain rate dependence of the fraction of plastic work converted into heat: an experimental study using high speed infrared detectors and the Kolsky bar. Mechanics of Materials 17, 135-145.

Mitchell, T.E., Spitzig, W.A., 1965. Three-stage hardening in tantalum single crystals. Acta Met., 1169-1179.

Mordike, B.L., Rudolph, G., 1967. Three-stage hardening in tantalum deformed in compression. J. Matls. Sc. 2, 332-228.

Regev, A., Rittel, D., 2008. Simultaneous transient temperature sensing of impacted polymers using infrared detectors and thermocouples. Exp. Mech. 48, 675-682.

Rittel, D., 1999. The conversion of plastic work to heat during high strain rate deformation of glassy polymers. Mechanics of Materials 31, 131-139.

Rittel, D., Bhattacharyya, A., Poon, B., Zhao, J., Ravichandran, G., 2007. Thermomechanical characterization of pure polycrystalline tantalum. Matls. Sc. and Engng. A A447, 65-70.

Rittel, D., Ravichandran, G., Venkert, A., 2006. The mechanical response of pure iron at high strain rates under dominant shear. Matls. Sc. and Engng. A A432, 191-201.

Taylor, G.I., Quinney, H., 1934. The latent energy remaining in a metal after cold working. Proc. Royal Soc. London 143, 607-326.

Zehnder, A.T., Guduru, P.R., Rosakis, A.J., Ravichandran, G., 2000. Million frames per second infrared imaging system. Review of Scientific instruments 71, 3762-3768.

FIGURES

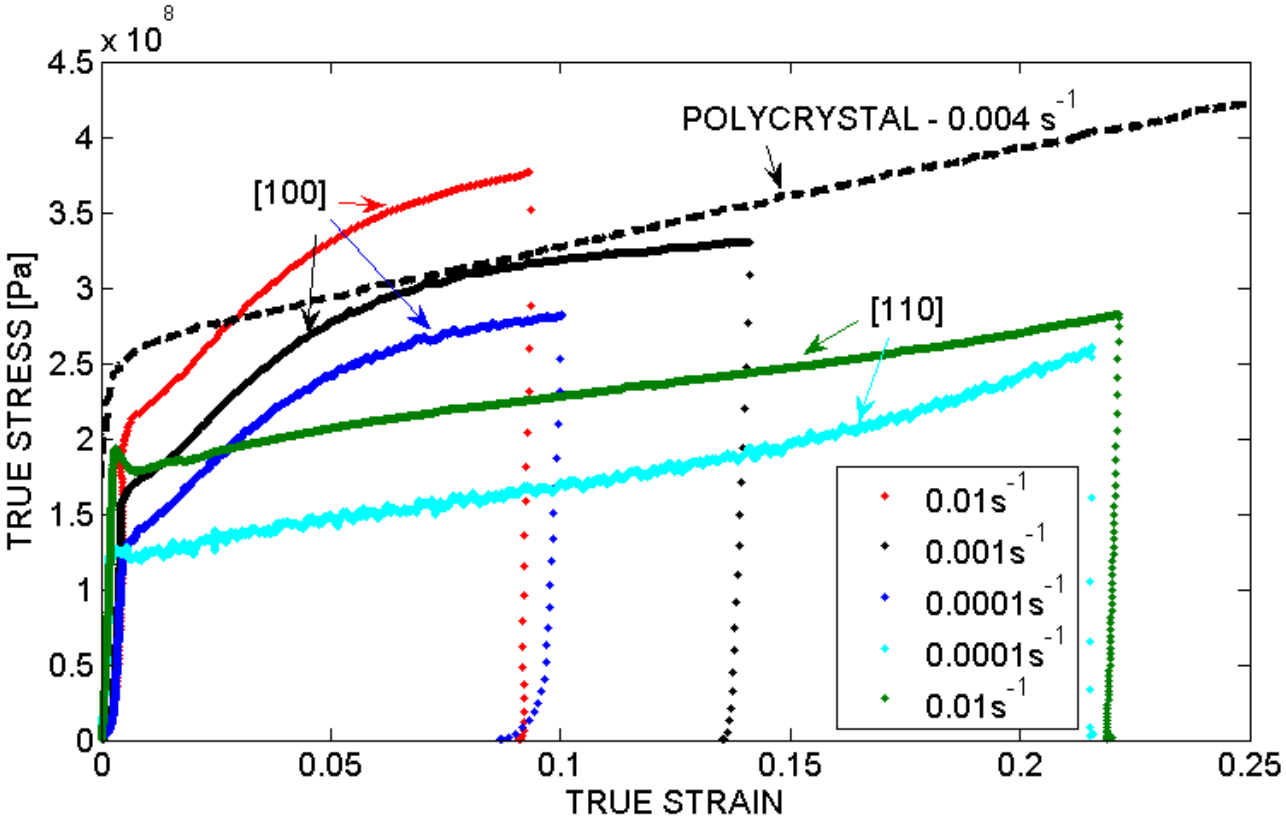

Figure 1: Quasi-static compression stress-strain curves of the [110] and [100] orientations. The flow curve of polycrystalline Ta is taken from Rittel et al. (2007). Note the similarity of [100] with the polycrystal.

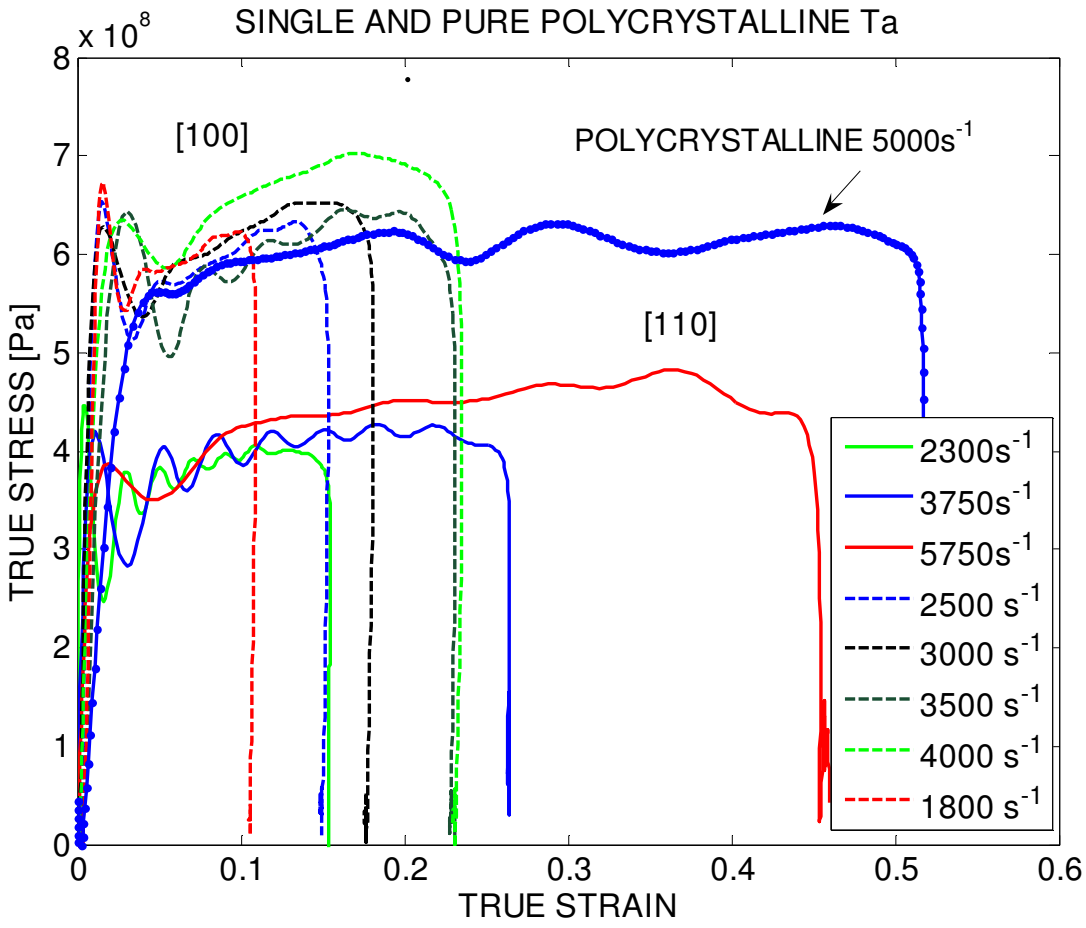

Figure 2: Dynamic compressive stress-strain curves of the [110] and [100] orientations. The flow curve of polycrystalline Ta is taken from Rittel et al. (2007). Note the similarity of [100] with the polycrystal.

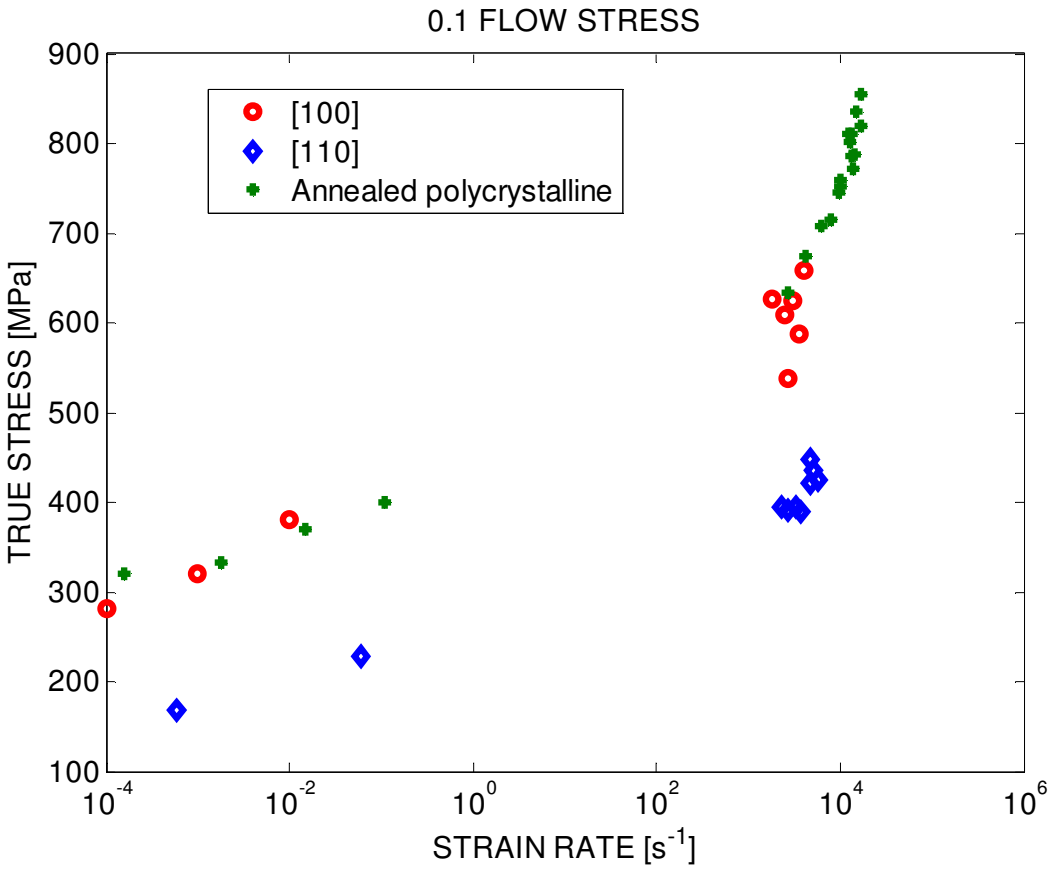

Figure 3: The rate sensitivity of [110] and [100] orientations at $\varepsilon = 0.1$. The data for polycrystalline Ta is taken from Rittel et al. (2007). Note the similarity of [100] with the polycrystal.

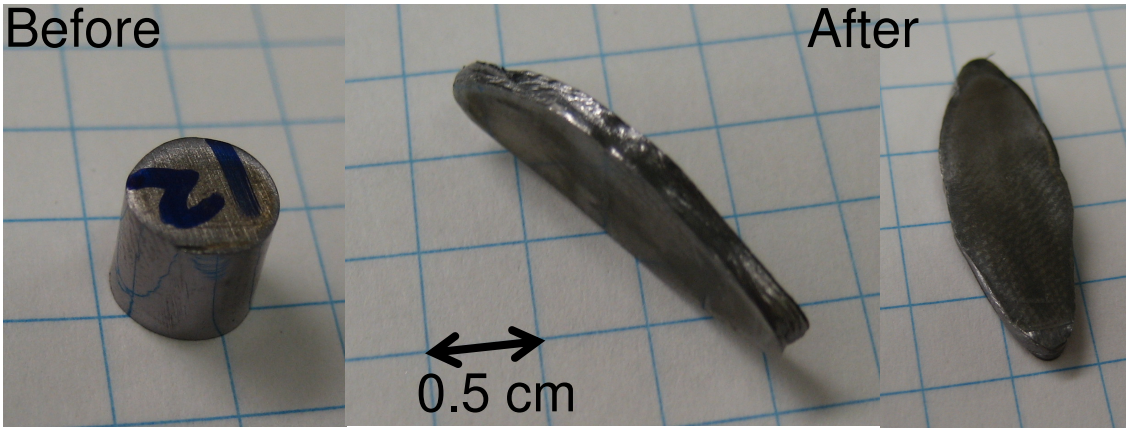

Figure 4: Typical shape of a [100] crystal before and after dynamic compression test.

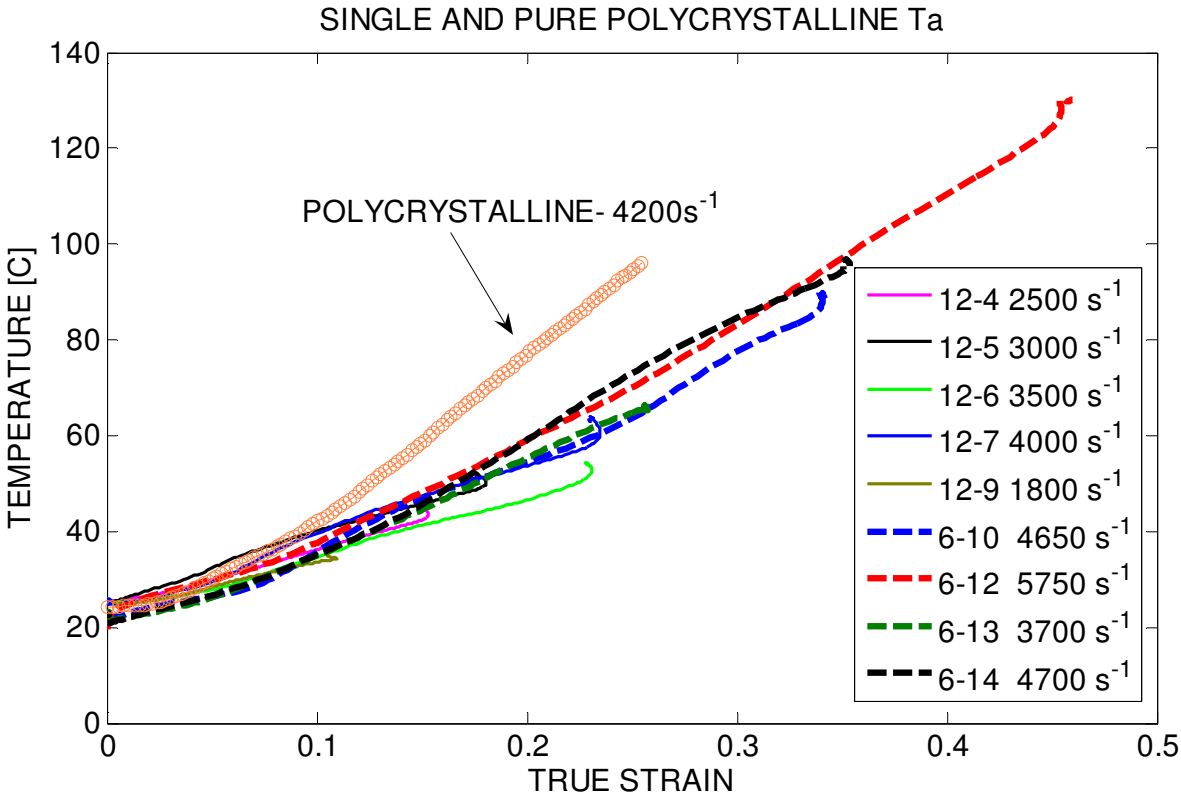

Figure 5: Typical temperature rise for the two orientations and polycrystalline Ta. Note the similarity of the curves for the single crystals, irrespective of the strain rate and orientation.

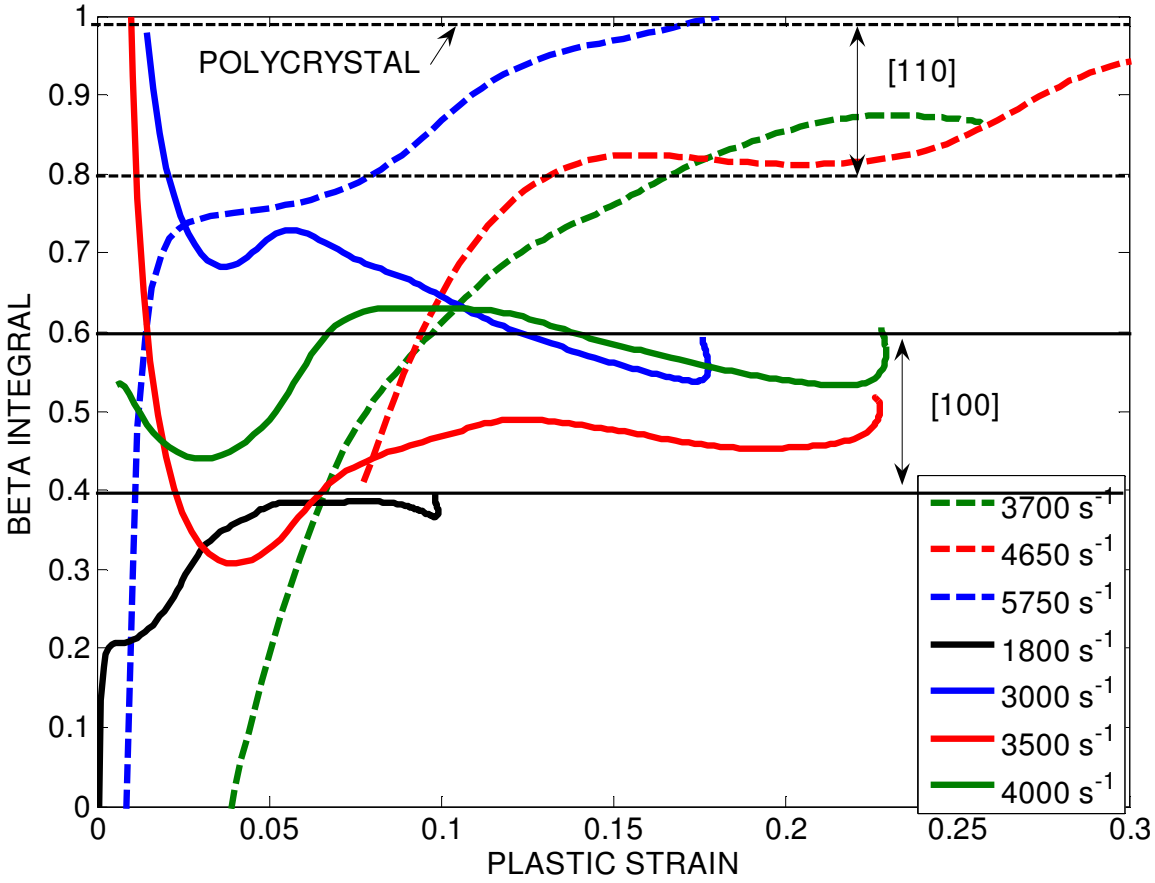

Figure 6: Typical evolution of the thermomechanical conversion factor - β_{int}. Note the different range of values for each orientation, with [110] tending to align with the polycrystalline curve for which β_{int} tends to 1.

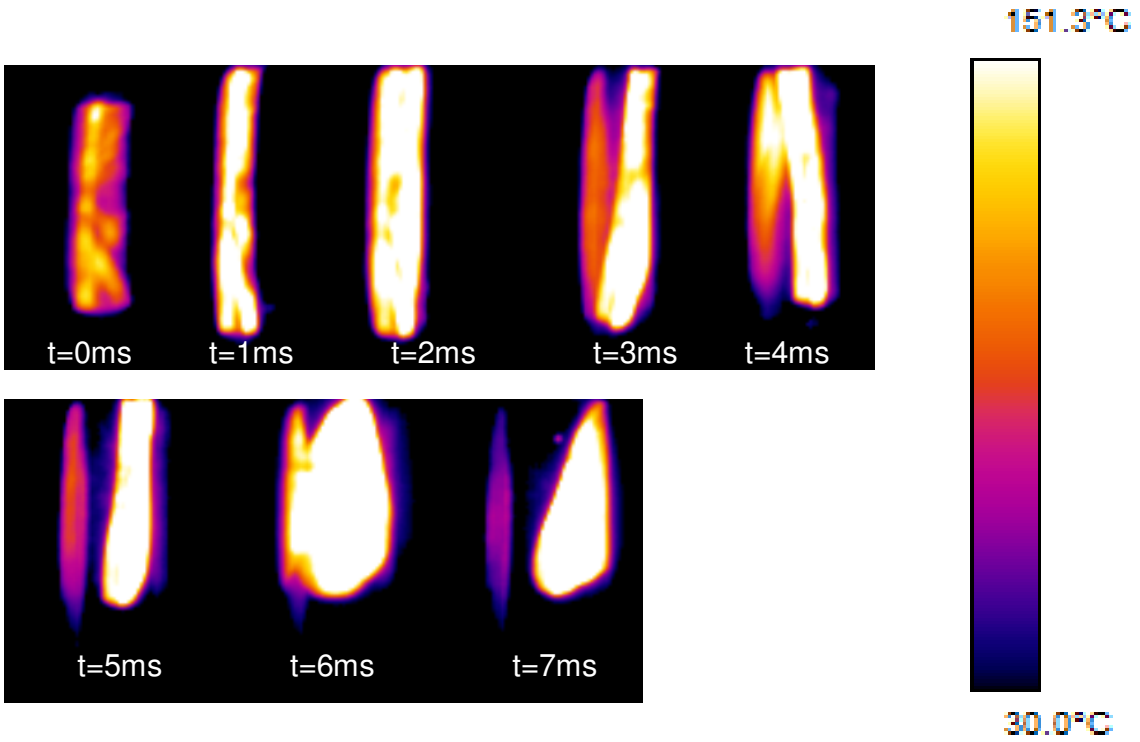

Figure 7: Temperature evolution of 6mm [100] recorded by the FLIR thermal camera. The temperature shown in the first frame (#0) is of the order of magnitude recorded by the infrared detector. However, the specimen remains clearly sandwiched between the bars in the next two frames and its temperature increases markedly as a result of repeated impact. The 4th and subsequent frames show the rigid body motion of the hot specimen. Note that the maximum recorded temperature is of the order of twice that recorded during the first impact (infrared detector).